AFGL-TR-78-0304
ENVIRONMENTAL RESEARCH PAPERS, NO. 648

LEVEL

A053164

Modeling of the Geosynchronous Orbit Plasma Environment — Part 2. ATS-5 and ATS-6 Statistical Atlas

HENRY B. GARRETT, Capt, USAF
E. G. MULLEN
E. ZIEMBA
S. E. DeFOREST

30 November 1978

DDC
APR 6 1979
RECEIVED
C

SPACE PHYSICS DIVISION   PROJECT 7661

AIR FORCE GEOPHYSICS LABORATORY

HANSCOM AFB, MASSACHUSETTS 01731
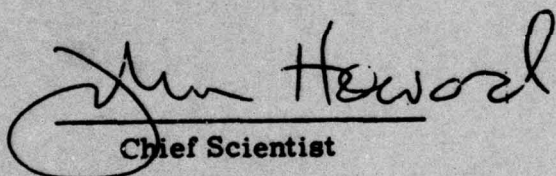
AIR FORCE SYSTEMS COMMAND, USAF

79 04 05 003

This report has been reviewed by the ESD Information Office (OI) and is releasable to the National Technical Information Service (NTIS).

This technical report has been reviewed and is approved for publication.

FOR THE COMMANDER

Chief Scientist

REPORT DOCUMENTATION PAGE		READ INSTRUCTIONS BEFORE COMPLETING FORM
1. REPORT NUMBER AFGL-TR-78-0304	2. GOVT ACCESSION NO. AFGL-ERP-648	3. RECIPIENT'S CATALOG NUMBER
4. TITLE (and Subtitle) MODELING OF THE GEOSYNCHRONOUS ORBIT PLASMA ENVIRONMENT. PART 2. ATS-5 AND ATS-6 STATISTICAL ATLAS.		5. TYPE OF REPORT & PERIOD COVERED Scientific. Interim.
		6. PERFORMING ORG. REPORT NUMBER ERP No. 648
7. AUTHOR(s) Henry B. Garrett, Capt. USAF E. G. Mullen, S. E. DeForest E. Ziemba		8. CONTRACT OR GRANT NUMBER(s)
9. PERFORMING ORGANIZATION NAME AND ADDRESS Air Force Geophysics Laboratory (PHG) Hanscom AFB Massachusetts 01731		10. PROGRAM ELEMENT, PROJECT, TASK AREA & WORK UNIT NUMBERS 76610803 62101F 98
11. CONTROLLING OFFICE NAME AND ADDRESS Air Force Geophysics Laboratory (PHG) Hanscom AFB Massachusetts 01731		12. REPORT DATE 30 November 1978
		13. NUMBER OF PAGES 34
14. MONITORING AGENCY NAME & ADDRESS(if different from Controlling Office) 35p.		15. SECURITY CLASS. (of this report) Unclassified
		15a. DECLASSIFICATION/DOWNGRADING SCHEDULE

16. DISTRIBUTION STATEMENT (of this Report)

Approved for public release; distribution unlimited.

17. DISTRIBUTION STATEMENT (of the abstract entered in Block 20, if different from Report)

Environmental research papers,

18. SUPPLEMENTARY NOTES

19. KEY WORDS (Continue on reverse side if necessary and identify by block number)

Spacecraft charging   Electrons
Geosynchronous environment   Ions
Energetic particles
Space physics
Environmental model

20. ABSTRACT (Continue on reverse side if necessary and identify by block number)

A preliminary statistical analysis of the ATS-5 and ATS-6 geosynchronous plasma data has been carried out. Variations in the electron and ion currents and temperatures, as represented by the single Maxwellian component temperatures T(AVG) and T(RMS), are evaluated with respect to local time and geomagnetic activity. The potential on the satellites is similarly evaluated. Results indicate that the geosynchronous plasma cannot be adequately represented by a simple Maxwellian distribution and that, at the very least, a two component Maxwellian is necessary. The electron current and eclipse potential were found

next page

409578

sub P

20.   (Cont)

to vary strongly with K_p while the temperatures only varied weakly. Local time variations in temperature and current were observed but these were outweighed by a significant local time variation in satellite potential which peaked near midnight. An explanation of these results is proposed in terms of a simple model of the time evolution of the plasma following an injection.

ACCESSION for

NTIS   White Section ☑
DOC   Buff Section ☐
UNANNOUNCED   ☐
JUSTIFICATION

BY
DISTRIBUTION/AVAILABILITY CODES
                          or SPECIAL

A

Preface

Many different people and organizations have contributed to this study. B. Johnson of UCSD reduced all of the ATS-6 data and potentials. C. McPhadden, also of UCSD, provided the computer tapes and spectrograms used in the study. C. Pike provided the motivation for the study. J. Fink drew many of the figures and provided significant analytic support. A. Lacroix of ASEC carried out most of the tape reduction. Our special appreciation, however, goes to R. McInerney of AFGL/SUA whose tireless, uncomplaining, and understanding assistance made the study possible. One of us (S. E. D.) would like to acknowledge support under contract F19628-77-C-0014.

3

Contents

Illustrations

Tables

Modeling of the Geosynchronous Orbit Plasma Environment – Part 2. ATS-5 and ATS-6 Statistical Atlas

1. INTRODUCTION

The quantitative statistical description of the geosynchronous plasma environment is an important issue from both an engineering and a scientific standpoint as it is necessary for the evaluation of the spacecraft charging phenomenon. At geosynchronous altitudes, which is the primary region of spacecraft charging, only a limited number of low energy (0-100 keV) plasma environment studies exist.[1,2,3,4,5] None of these studies have detailed together the statistical occurrence of electron and ion temperatures, currents and, of particular concern to the engineering community, spacecraft potentials (see, however, References 6, 7, and 8). These parameters constitute the minimum set of quantities considered necessary to model the effects of the ambient environment on space charge buildup. This report presents a detailed statistical analysis of these parameters as determined from data recorded by the ATS-5 and ATS-6 geosynchronous satellites. Particular emphasis is placed on the needs of the spacecraft charging community.

Firstly, this report reviews the satellites and instrumentation that provided the data. Next, the problems involved in defining the ambient temperatures, satellite potentials, and ambient currents to the spacecraft are discussed. The statistical

distributions of these quantities are then presented. The ATS-5 and ATS-6 data are compared, and results of a study of the local time and geomagnetic activity variations of the potential, currents, temperatures, and their joint probability of occurrence are given. A simple quantitative model is then advanced in order to explain the results.

2. DATA BASE

The University of California at San Diego (UCSD) plasma experiments on the geosynchronous satellites ATS-5 and ATS-6 were the data sources for this study. Although a brief description of both satellites and instruments is given, the reader is referred to DeForest and McIlwain[2] for a more detailed description of ATS-5 and Mauk and McIlwain[9] for ATS-6. This section also describes the type of data returned and discusses some of the uncertainties in the data. The primary data used for this study are the 10-min averages for the 50 days of ATS-5 and 46 days of ATS-6 data listed in Table 1. Also listed are the 3-hr K_p values of geomagnetic activity for the same time period.

The ATS-5 satellite was launched into geosynchronous orbit in August 1969. Since September of 1969 it has been maintained near 105°W and at an inclination of 2.3°. It is currently spinning with its spin axis parallel to the earth's at a rate of 0.79 sec/cycle. ATS-5 is a right circular cylinder having dimensions of 1.8 m in length and 1.5 m in diameter. Two pairs of electron and positive ion cylindrical plate spectrometers (that is, electrostatic or ESA detectors) are directed parallel and perpendicular to the spin axis. The ATS-5 plasma experiment measured the particle population between 51 eV and 51 keV in 64 energy steps (2 background channels and 62 logarithmically spaced energy channels) in 20 seconds. The energy steps are each 112 percent of the previous step giving an approximation digitization error of ± 5 percent.

The ATS-6 satellite was launched into geosynchronous orbit in May 1974. Initially, the satellite was located at 94°W longitude with an inclination of 2.5° (the 1974 measurements were made at this position). Subsequently, the satellite was moved to 107°E longitude where the 1976 measurements were made. The ATS-6 satellite differs fundamentally in shape from the ATS-5 satellite. It is essentially a 10-m diameter dish antenna. The UCSD instrument is located on the back of the antenna and, as the satellite is 3-axis stabilized, designed to rotate. For the data reported here, however, only the so-called north-south pointing electron and ion detector pair, when they were stationary, are considered. The detectors are basically the same design as those on ATS-5, but the energy range is 0-80 keV, with a 16-sec cycle and energy step size of ~113 percent.

9. Mauk, B.H., and McIlwain, C.E. (1975) ATS-6 UCSD auroral particles experiment, IEEE Trans. Aerospace and Electronics Systems, AES-11(No. 6):1125-1130.

Table 1. Days for Which ATS-5 and ATS-6 Data Were Obtained. Also shown are the 3-hr geomagnetic indices for the same days. The conversion values to K_p (or a_p) are: $0 = 0_o$, $1 = 0+ (=2)$, $2 = 1 - (=3)$, ..., and $27 = 9_o (=400)$

ATS-5

YEAR DAY	3 HOUR GEOMAGNETIC INDICES							

ATS-6

YEAR DAY	3 HOUR GEOMAGNETIC INDICES							

The data consist of differential count rates as a function of time. As described below, these count rates are converted to differential flux spectra from which the ambient currents and temperature can be determined. The spectra also directly reveal the satellite potential. Briefly, the low energy ion (electron) population is accelerated if the satellite is charged negative (positive) with respect to the ambient plasma. This produces a pronounced cut-off in the ion (electron) spectra immediately below the energy channel corresponding to the satellite potential. Thus, independent of the characteristics of the ATS-5 and ATS-6 detectors, the satellite potential can be determined.

3. THE DISTRIBUTION FUNCTION

As demonstrated in Garrett,[4] the plasma distribution function (or phase-space density) F is the most widely accepted function for describing the plasma. Mathematically, F is given by:

$$F(X, Y, Z, V_X, V_Y, V_Z) \tag{1}$$

such that

$$F(X, Y, Z, V_X, V_Y, V_Z) \, dX \, dY \, dZ \, dV_X \, dV_Y \, dV_Z$$

is the number of particles in the velocity space $dV_X \, dV_Y \, dV_Z$ and the spatial volume $dX \, dY \, dZ$ where

X, Y, Z = spatial coordinates

and

V_X, V_Y, V_Z = velocity components.

Assuming that the plasma is isotropic and Maxwellian, in spherical coordinates

$$F(X, Y, Z, V_X, V_Y, V_Z) = f(X, Y, Z, V) \, 4\pi \, V^2 \, dV$$

where

10

$$V = (V_X{}^2 + V_Y{}^2 + V_Z{}^2)^{1/2} \,,$$

$f(V_i)$ = isotropic Maxwellian distribution function

$$= n_i \left(\frac{m_i}{2\pi k T_i} \right)^{3/2} e^{-m_i V_i{}^2/2kT_i} \,,$$

n_i = number density of species i,

m_i = mass of species i,

T_i = temperature of species i,

V_i = velocity of species i,

k = Boltzmann constant.

Taking the first four moments[4] we find

$$\langle N_i \rangle = 4\pi \int_0^\infty (V^0) f_i V^2 \, dV = n_i \tag{2}$$

$$\langle NF_i \rangle = \int_0^\infty (V^1) f_i V^2 \, dV = \frac{n_i}{2\pi} \left(\frac{2kT_i}{\pi m_i} \right)^{1/2} \tag{3}$$

$$\langle EN_i \rangle = 4\pi \left(\tfrac{1}{2} m_i \right) \int_0^\infty (V^2) f_i V^2 \, dV = 3/2 \, nkT_i \tag{4}$$

$$\langle EF_i \rangle = \left(\tfrac{1}{2} m_i \right) \int_0^\infty (V^3) f_i V^2 \, dV = \frac{m_i n_i}{2} \left(\frac{2kT_i}{\pi m_i} \right)^{3/2} \tag{5}$$

where

$\langle N_i \rangle$ = number density for species i (number/cm^3),

$\langle NF_i \rangle$ = number flux for species i (number/cm^2-sec-sr),

$\langle EN_i \rangle$ = energy density (eV/cm^3),

$\langle EF_i \rangle$ = energy flux for species i (eV/cm^2-sec-sr).

11

As described in Garrett,[4] the four moments can be derived directly from the differential flux spectra. Garrett also demonstrates that the distribution function or the four moments (unlike the plasma temperature, T_i) can be averaged together to give a physically meaningful average quantity. We can define a two Maxwellian distribution function f_{2i} (that is, the sum of two distinct Maxwellian plasma components for a single particle species) in terms of the densities n_{1i} and n_{2i} and the temperature T_{1i} and T_{2i},

$$f_{2i}(V_i) = \left(\frac{m_i}{2\pi k}\right)^{3/2} \left(\frac{n_{1i}}{T_{1i}^{3/2}} \; e^{-m_i V_i^2/2kT_{1i}} + \frac{n_{2i}}{T_{2i}^{3/2}} \; e^{-m_i V_i^2/2kT_{2i}} \right). \tag{6}$$

The plasma "temperature", if the plasma is described by a <u>single</u> Maxwellian, is easily obtainable from Eqs. (2-5) by

$$T_i(AVG) = \frac{2}{3} \frac{\langle EN_i \rangle}{k \langle N_i \rangle} = T_i, \tag{7a}$$

$$T_i(RMS) = \frac{1}{2} \frac{\langle EF_i \rangle}{k \langle NF_i \rangle} = T_i, \tag{7b}$$

$$T_i(AVG) = T_i(RMS). \tag{7c}$$

If, however, the plasma consists of two or more components such as described by Eq. (6), we find

$$T_i(AVG) = \frac{2}{3} \frac{\langle EN_i \rangle}{k \langle N_i \rangle} = \frac{n_{1i} T_{1i} + n_{2i} T_{2i}}{n_{1i} + n_{2i}}, \tag{8a}$$

$$T_i(RMS) = \frac{1}{2} \frac{\langle EF_i \rangle}{k \langle NF_i \rangle} = \frac{n_{1i} T_{1i}^{3/2} + n_{2i} T_{2i}^{3/2}}{n_{1i} T_{1i}^{1/2} + n_{2i} T_{2i}^{1/2}}. \tag{8b}$$

So that in general

$$T_i(AVG) \neq T_i(RMS). \tag{8c}$$

This represents a serious dilemma in defining the temperature. A description of the plasma in terms of n_1, n_2, T_1, and T_2 is thus preferable to either T(AVG) or T(RMS). Unfortunately, few of the existing spacecraft charging codes can input more than a single Maxwellian. Technically, since T(AVG) is the mean energy of the particle distribution, it is the preferable definition if a single temperature is desired. It does not necessarily give the "best" estimate of the potentials since

12

it is always less than T(RMS) which may be the more conservative estimate. In this report we will compare T(AVG) and T(RMS). Their difference is a measure of the deviation of the plasma from a single Maxwellian. It must be remembered, however, that they do not provide an accurate description of the plasma.

The current to the spacecraft (actually the current per unit area) is the other quantity most often required for potential calculations. Unlike the temperature, the current, J_i, can be derived directly from the four moments,[4]

$$J_i = q_i \int_0^\infty V_i \cdot \vec{n} f d^3 V \qquad (9)$$

$$= \pi q_i \langle NF_i \rangle$$

where

$\vec{n}$ = unit normal to area,

q_i = charge on species (C),

J_i = current per unit area (A/cm^2).

This assumes the particle flux to be omnidirectional. If, as is observed on occasion, the plasma flux is directional, then the integral of Eq. (9) would not be exactly $\pi q \langle NF_i \rangle$ (observations indicate that the correction factor is of the order of unity)—a factor that should be taken into account in considering our results.

4. RESULTS

4.1 Introduction

As outlined in Garrett[4] the differential energy flux was integrated to give the four moments defined in Eqs. (2-5). These in turn were averaged for ATS-5 and ATS-6 to give 10-min averages. The ATS-5 data for the parallel and perpendicular detectors (from the UCSD master tapes) were averaged together. It was this data base of approximately 50 days of ATS-5 and ATS-6* plasma data that was then analyzed. T(AVG) and T(RMS) were calculated from these data assuming Eqs. (7a) and (7b).

---

*The ATS-6 data were contaminated by a large photoelectron return current and large differential potentials. An attempt was made to correct for these effects but errors still remain so the ATS-6 data must be considered provisional.

13

The potential data, although also from ATS-5 and ATS-6, were obtained in a different manner. For eclipses, the potential was measured at 10-min intervals during each eclipse in the 1969-1972 time frame for ATS-5. Only one eclipse period (spring 1976) was available for ATS-6. Daylight potential values were provided only on the ATS-6 data tape and at approximately 16-sec intervals (see Johnson and Whipple, 1978, for a description of original tape). These were averaged to give 10-min values.

In this section, using the data base just defined, we will seek to describe T(AVG), T(RMS), the current, and the potential in terms of three variations:

(1) Statistical distribution—that is, a histogram of the occurrence frequency of the parameter as a function of its amplitude,

(2) Local time variation—the occurrence frequency as a function of local time and amplitude,

(3) Geomagnetic variations—the occurrence frequency as a function of the geomagnetic activity index K_p.

The current and temperature are also intercompared and a simple model advanced that attempts to explain the observed relationships. Further, ATS-5 and ATS-6 data are compared and contrasted in order to draw a consistent picture of the geosynchronous orbit. It should be noted, however, that ATS-5 and ATS-6 do not sample identical regions of space as their orbits are not identical. Hence, some differences, particularly in local time variation, are expected.

4.2 Statistical Distribution

The simplest analysis of a variable that can be accomplished is to plot the occurrence frequency of different values of the variable. Figure 1 shows the occurrence frequencies of various values of T(AVG), T(RMS), and current for electrons and ions for both ATS-5 and ATS-6. All distributions can be described in terms of standard statistical distributions for data randomly distributed around some mean (that is, either a Poisson or Gauss distribution). Table 2 lists approximate averages and standard deviations for each distribution. [*]

---

[*]Note: As previously discussed, the ATS-6 values are provisional.

14
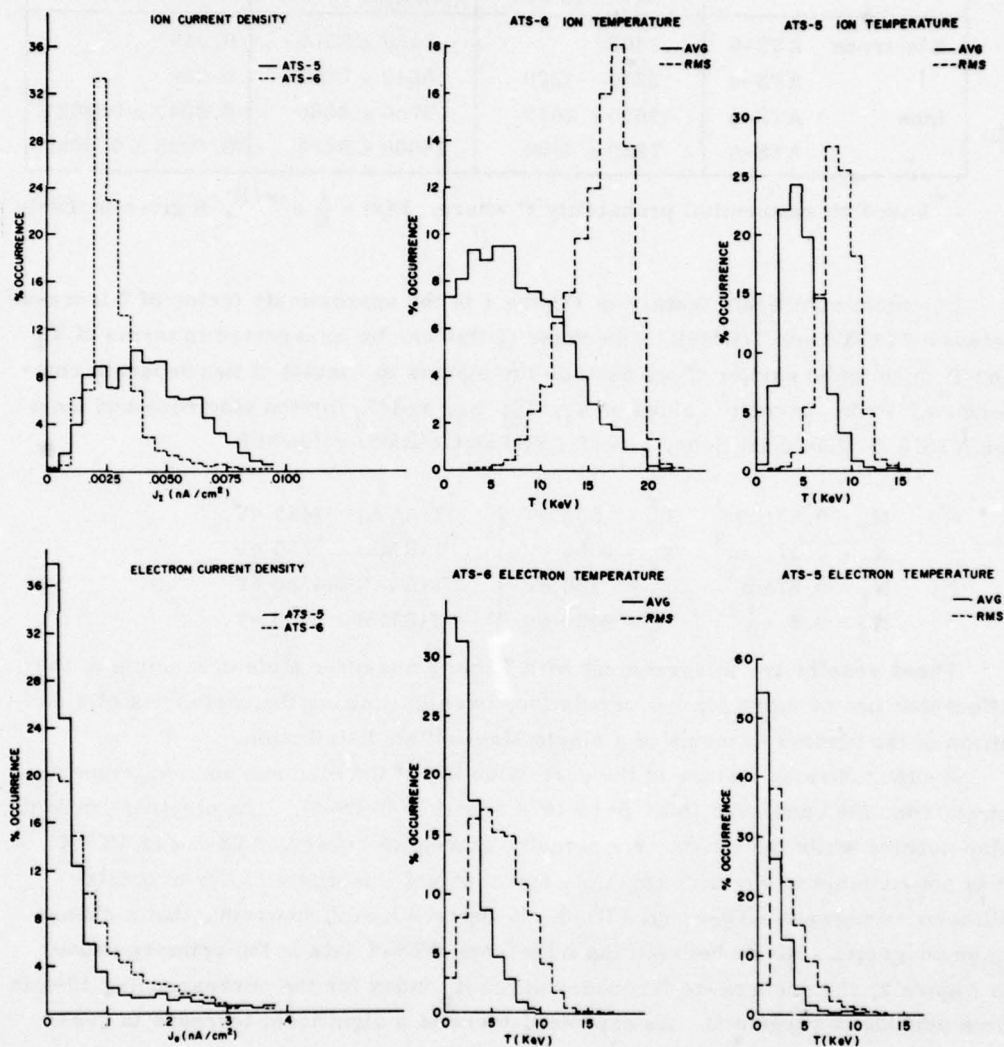
Figure 1. Occurrence Frequencies of T(AVG), T(RMS), and Current for the Geosynchronous Electron and Ion Plasma Measured by ATS-5 and ATS-6. The ATS-6 results are provisional

15

Table 2. Average and Standard Deviations for T(AVG), T(RMS), and the Current for the Geosynchronous Electron and Ion Plasma Populations Measured by ATS-5 and ATS-6. The ATS-6 data are provisional

		T(AVG) in keV	T(RMS) in keV	J in n A/cm^2
Electrons	ATS-5	1500*	3480 ± 2070	0.045*
	ATS-6	2290 ± 1800	5640 ± 2700	0.08*
Ions	ATS-5	5030 ± 2010	8750 ± 1860	0.0043 ± 0.0021
	ATS-6	7880 ± 4900	16000 ± 3400	0.0026 ± 0.0012

*Based on exponential probability P where: $P(x) = \frac{1}{B} e^{-x/B}$, B given in Table 2.

The most significant feature of Figure 1 is the approximate factor of 2 increase between T(AVG) and T(RMS). The cause of this can be interpreted in terms of T_1 and T_2 mentioned earlier if we assume the plasma to consist of two separate components. From Garrett[4] values of N_1, T_1, N_2, and T_2 for the electrons and ions, for ATS-5 median conditions, give T(AVG) and T(RMS) values of:

$$e^-: \quad N_1 = 0.83/cm^3 \quad T_1 = 500 \text{ eV} \quad\} \quad T(AVG) = 1435 \text{ eV}$$
$$N_2 = 0.17/cm^3 \quad T_2 = 6000 \text{ eV} \quad T(RMS) = 2780 \text{ eV}$$
$$I^+: \quad N_1 = 0.5/cm^3 \quad T_1 = 100 \text{ eV} \quad\} \quad T(AVG) = 4550 \text{ eV}$$
$$N_2 = 0.5/cm^3 \quad T_2 = 9000 \text{ eV} \quad T(RMS) = 8150 \text{ eV}.$$

These results are in agreement with Table 2 and offer a clear example of the effect that two or more plasma populations have in limiting the usefulness of a definition of the plasma in terms of a single Maxwellian distribution.

Another obvious feature is the near-doubling of the electron and ion temperatures from 1969 and 1970 (ATS-5) to 1974 and 1976 (ATS-6). The electron current also doubles while the ion current actually decreases between ATS-5 and ATS-6. It is not possible to say with certainty how much of this effect is due to orbital differences between ATS-5 and ATS-6. It appears likely, however, that a change in geomagnetic activity between the ATS-5 and ATS-6 data is the primary cause. In Figure 2, the occurrence frequency of the K_p index for the corresponding 10-min time periods is presented. As expected, there is a significant increase in geomagnetic activity from ATS-5 to the ATS-6 time frame.

In Figures 3 and 4 we have plotted the occurrence frequency of the potential. Figure 3 is for ATS-6 daylight charging events only (note: the plot is only for the 1026 charging intervals and does not include the 5242 zero potential intervals). Figure 4, which is a plot of the occurrence frequency of the potential during eclipse, is binominal (Note: 0 potential values are included in this figure). The primary

16
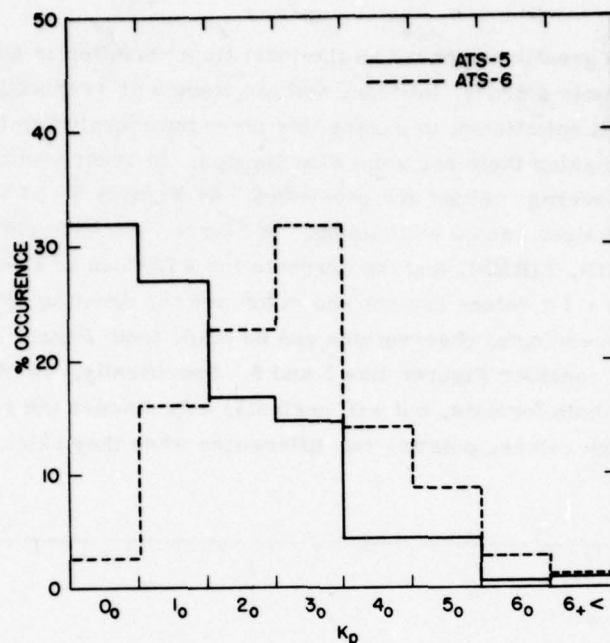
Figure 2. Occurrence Frequency of the Geomagnetic
Index K_p for the 10-min Intervals of ATS-5 and ATS-6
Used in the Analysis

cause of this is not known though a possible explanation is that there is a critical
electron temperature for charging to occur (see Garrett and Rubin).[10]   Figure 4
also supports the previous observations that the electron temperature of the plasma
has doubled between the time of the ATS-5 and the ATS-6 observations as the
electron temperature is roughly proportional to the potential on the satellite (see
Garrett and Rubin).[10]   This does not, however, rule out a change in plasma due
to different orbits rather than geomagnetic activity.

4.3 Local Time Variation

Of critical importance to mission planning as regards spacecraft charging
(particilarly differential charging) is the local time variation of the plasma and
potential. There are, however, several problems in studying these variations.
Figures 5 and 6 are occurrence frequency plots of T(AVG) as a function of local time
for the electrons as observed by ATS-5 and ATS-6 (these are examples of contour
plots where the contours are at intervals of constant percentage). The interpreta-

10. Garrett, H.B., and Rubin, A.G. (1978) Spacecraft Charging at Geosynchronous
      Orbit-solution for Eclipse Passage, AFGL-TR-78-0122.

17

tion of such plots is greatly hampered as the local time variation is a simultaneous function of geomagnetic activity, latitude, and longitude with respect to the earth (in this study we will not attempt to pursue this issue but merely remind the reader of its importance) making their use somewhat limited. In order to simplify the presentation, only average values are presented. As Figures 5 and 6 indicate, however, average values can be misleading. In Figure 7 we have plotted the average values of T(AVG), T(RMS), and the currents for ATS-5 and ATS-6 as a function of local time. The ± 1 σ values are not shown but are the order of those given in Table 2. Several meaningful observations can be made from Figure 7 provided we are careful to also consider Figures like 5 and 6. Specifically, we have plotted all the functions in both formats, but will normally only discuss the results in terms of the average values, pointing out differences when they exist.
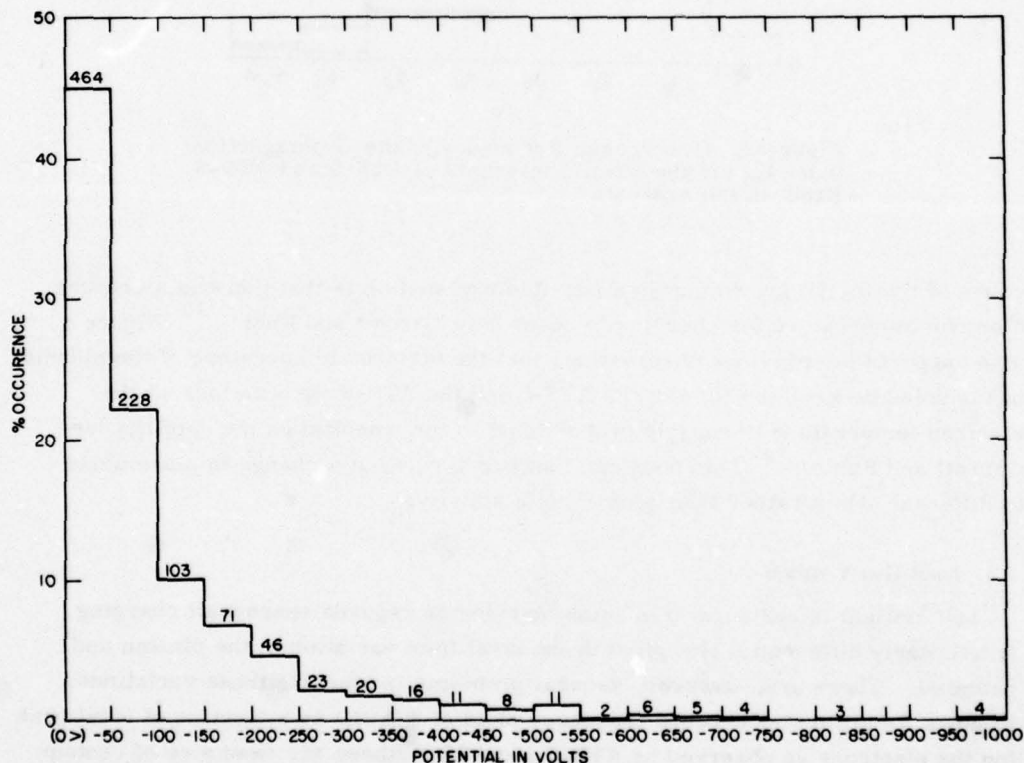
Figure 3. Occurence Frequency of Non-zero Potentials for ATS-6 When in Sunlight. (Note: Percent is for total of non-zero values — that is, 1026 values out of 6268 total observations)

18
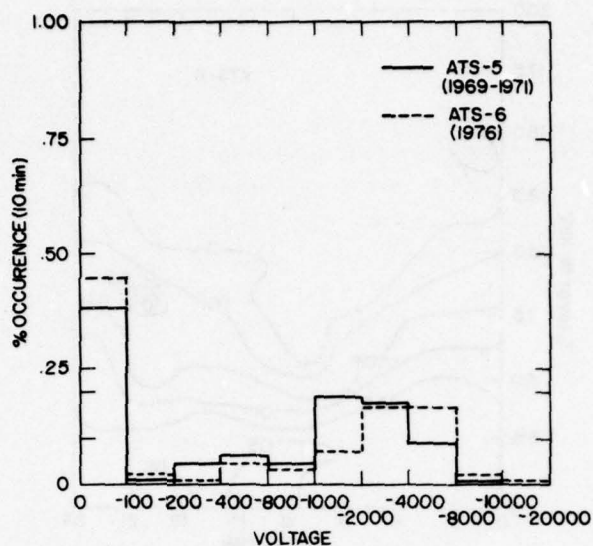
Figure 4. Occurence of Frequency of ATS-5 (1969-1972) and ATS-6 (1976) Eclipse Potentials (10-min intervals)
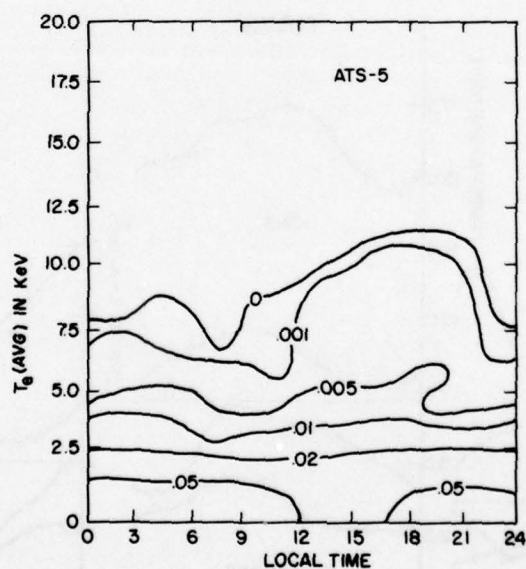
Figure 5. Contour Plot of Occurrence Frequency of T(AVG) as a Function of Local Time and Amplitude for the Electron Data From ATS-5. Contours correspond to percentage of _all_ 10-min intervals studied

19
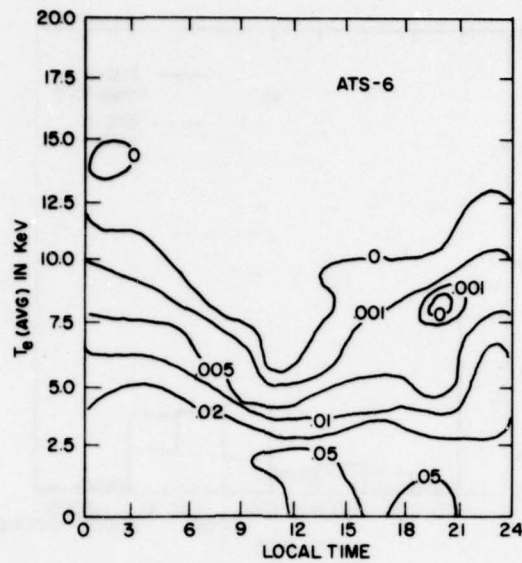
Figure 6. Same as Figure 5 for ATS-6
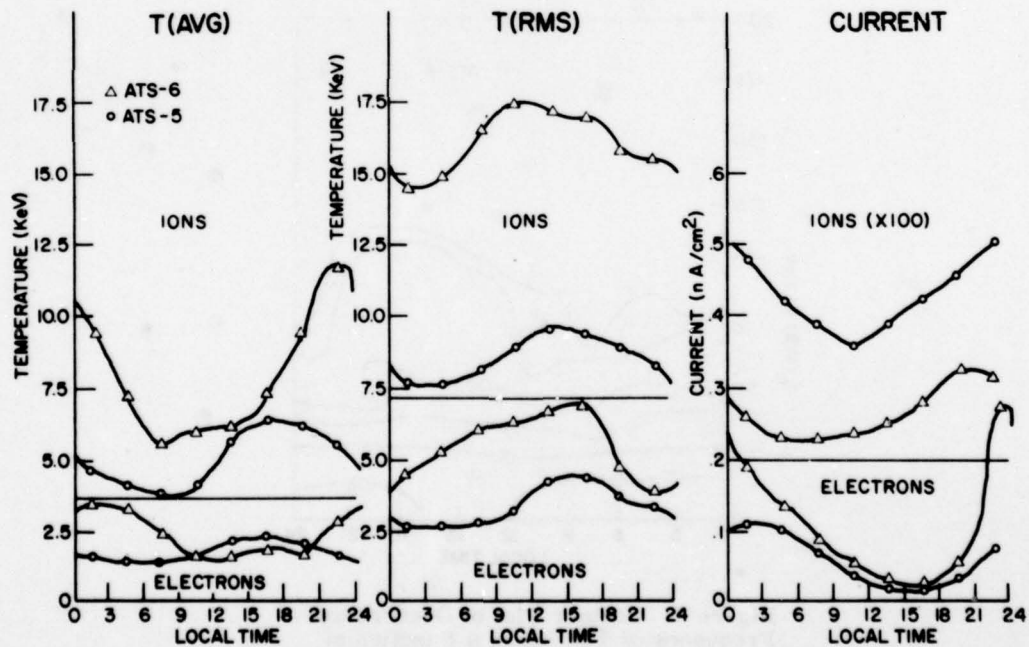
Figure 7. The Average Values of T(AVG), T(RMS), and Current as Functions of Local Time for ATS-5 and ATS-6 (the ATS-6 data are provisional)

20

Returning to the data, Figure 7 for the T(RMS) temperatures shows agreement between the ATS-5 and ATS-6 data which is evident in the corresponding contour plots. The electron temperatures peak near 1500-1600 LT and reach minimum between 2100-0300 LT. The ions peak near 1000-1500 and reach minimum between 0300-0600 LT. Unlike T(RMS), T(AVG) is not consistent between ATS-5 and ATS-6. In fact, T(AVG) for ATS-5 is roughly in phase with T(RMS) whereas T(AVG) for ATS-6 is 12 hr out of phase. The contour plots for T(AVG), however, show somewhat better qualitative agreement between the electron T(AVG) for ATS-5 and ATS-6 than the average values indicate. Similarly, the contour plot for the ions show agreement. The reason for the disagreement between the average plots and the contour plots is not apparent but can be traced to the division of the plasma into several distinct components following injection (see later).

In Figure 7 good agreement exists between the ATS-5 and ATS-6 ion and electron current data which is also reflected in their contour plots. The electron currents minimize between 1500-1800 LT and peak between 2100-0300 LT. The ion currents peak between 1800-2400 LT and minimize between 0600-1200 LT. The factor of ~50 difference between the levels of the electron and ion currents is due to the mass difference between the ions and electrons which enters the equation for the current as the square root of the masses.

The average potential as a function of local time for daytime charging is shown in Figure 8. The dots correspond to the average values (only for non-zero values) in the respective intervals. Unlike the other parameters, there is a pronounced local time variation peaking near midnight. This local time variation was revealed in the same data earlier, [5, 6, 8] and is known to be anti-correlated with encounters of the low-energy plasmasphere.
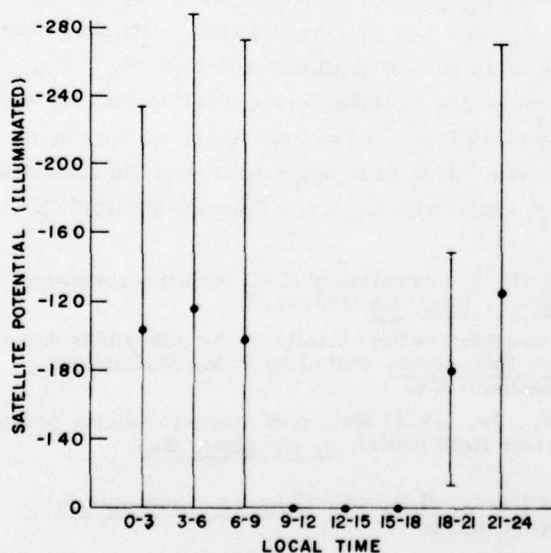
Figure 8. Average Potential as a Function of Local Time for ATS-6. The averages correspond to only the 1026 10-min values for which a potential was observed

21

4.4 Variation With Geomagnetic Activity

Geomagnetic activity and the phenomena related to it are believed to occur in association with the injection of hot plasma at geosynchronous orbit. [1, 2, 11] The subsequent dispersion of the plasma cloud[12, 13] forms a very important area in the study of magnetospheric physics. For the engineer or mission planner, the details of the process are not important. Primarily they desire information on the outcome—that is, how does geomagnetic activity change, on the average, the conditions at geosynchronous orbit. Unfortunately, a satellite at geosynchronous orbit exists in a three-dimensional volume and any movement of the magnetosphere in response to geomagnetic activity (see Garrett et al)[14] is liable to carry the satellite into widely differing plasma regions. On the whole, a geosynchronous satellite is believed to move from a relatively cold, dense plasma (the plasmasphere) into a hot, less dense plasma (the plasmasheet) during magnetic storms. At such times the satellite can find itself in magnetospheric regions containing almost no plasma (the high latitude tail) or even in the solar wind. This greatly confuses any attempt at a statistical analysis and only in the sense of a detailed magnetospheric model can we hope to understand such phenomena. Such a study will be left to a future report. For this report only geomagnetic variations in the current, temperature, and potential in statistical terms will be discussed. We realize that for this variation in particular such a method is less meaningful and that large error bars are to be expected.

In Figures 9 through 12 we have plotted the averages of the temperatures and currents as a function of the 3-hr geomagnetic K_p index. None of the temperatures or current show a simple dependence on K_p. There is, however, a trend for the current and T(AVG) to increase with K_p. As this may be in part an artifact of the occurrence frequency of K_p (Figure 2), it is best to exclude the data for $K_p \gtrsim 5_+$. Once this is done, the electron current shows a strong linear relation with K_p and excellent agreement between ATS-5 and ATS-6. The temperature, on the other hand, still shows only a weak correlation. This is in agreement with the simulation model[4] which predicts a significant increase with K_p of the ion and, particularly,

11. Mauk, B.H., and McIlwain, C.E. (1974) Correlation of K_p with the substorm plasma sheet boundary, J. Geophys. Res. 79:3193-3196.

12. McIlwain, C.E. (1972) Plasma convection in the vicinity of the geosynchronous orbit, in Earth's Magnetospheric Processes, edited by B.M. McCormac, p 268, D. Reidel, Dordrecht, Netherlands.

13. Roederer, J.G., and Hones, E.W., Jr. (1974) Motion of magnetospheric particle clouds in a time-dependent electric field model, J. Geophys. Res. pp 1932-1438.

14. Garrett, H.B., Pavel, A.L., and Hardy, D.A. (1977) Rapid Variations in Spacecraft Potential, AFGL-TR-77-0132.

the electron currents, a slight increase in T(AVG) for the electrons, and no increase in T(AVG) for the ions or in T(RMS) for either species. Any interpretation is complicated, however, by the above mentioned problem of the possible movement of widely different regions over the satellite and by the added complication of whether K_p is even an adequate indicator of geomagnetic activity at geosynchronous altitudes (a point we will not pursue in this report).

The potential variations with geomagnetic activity are likewise subject to the changes in the magnetospheric regions. In Figures 13 and 14 we have plotted the average potential for charging events (daylight or eclipse) as a function of K_p. The eclipse data, which represent a much more localized region of space (namely within a few degrees of local midnight), show a significant linear correlation with geomagnetic activity even though the error bars are very large. The daylight charging events which were previously shown to be localized in the midnight-dawn quadrant, also increase with geomagnetic activity. The coarseness (3-hr resolution) of the K_p index hampers this interpretation as changes in plasma and the potential can take place in seconds. Even so, an explanation in terms of the observed temperature and current variations[15] adequately explains these variations.

15. Rubin, A. G., Garrett, H. B., and Rothwell, P. L. (1978) ATS-5 and ATS-6 potentials during eclipse, Proceedings of the Second Spacecraft Charging Technology Conference (to appear as AFGL/NASA publication).
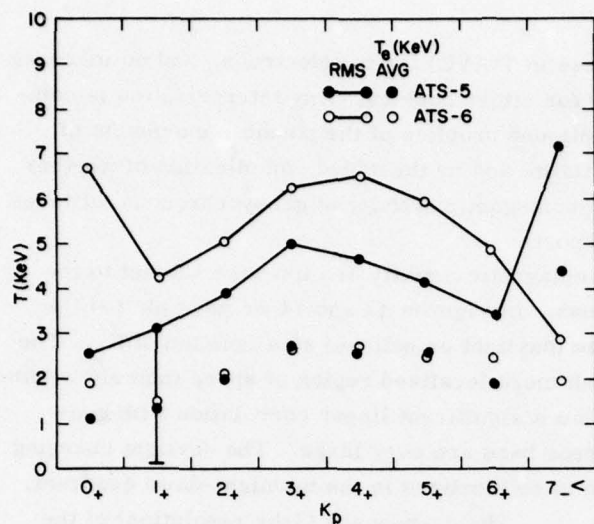
Figure 9. The Average Electron Temperature [T(AVG) and T(RMS)] for ATS-5 and ATS-6 as a Function of the K_p Intervals Indicated. A typical error bar is indicated
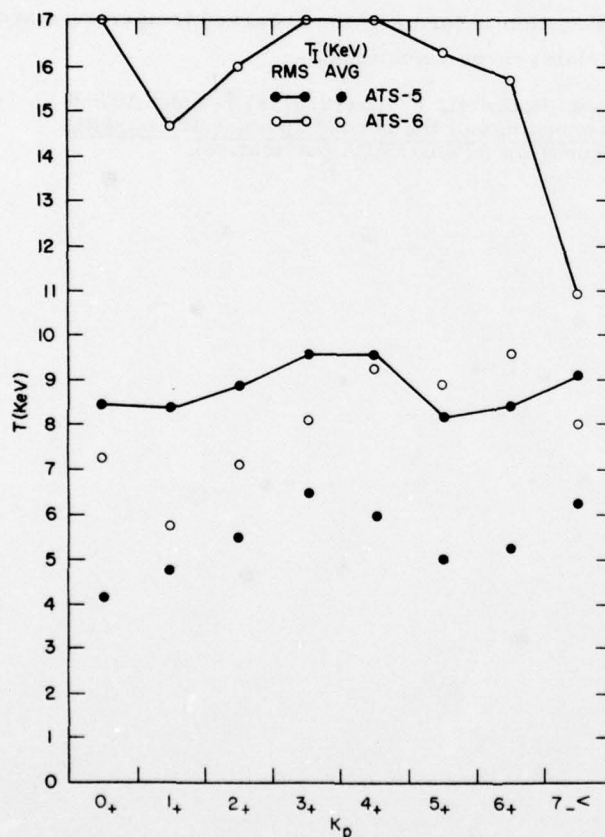
Figure 10. The Average Ion Temperature [T(AVG) and T(RMS)] for ATS-5 and ATS-6 as a Function of the K_p Intervals Indicated. A typical error bar is indicated

24
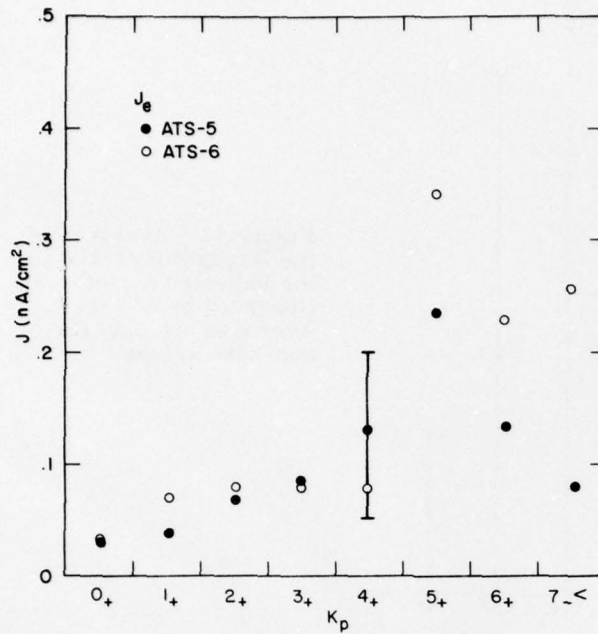
Figure 11. The Electron Current, J_e, for ATS-5 and ATS-6 as a Function of the K_p Intervals Indicated. A typical error bar is indicated
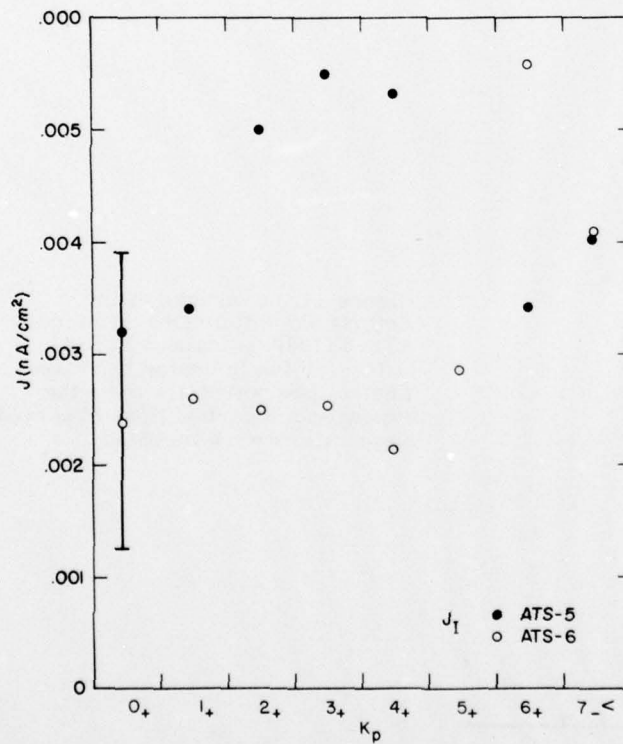
Figure 12. Same as Figure 11 for the Ion Current, J_I

25
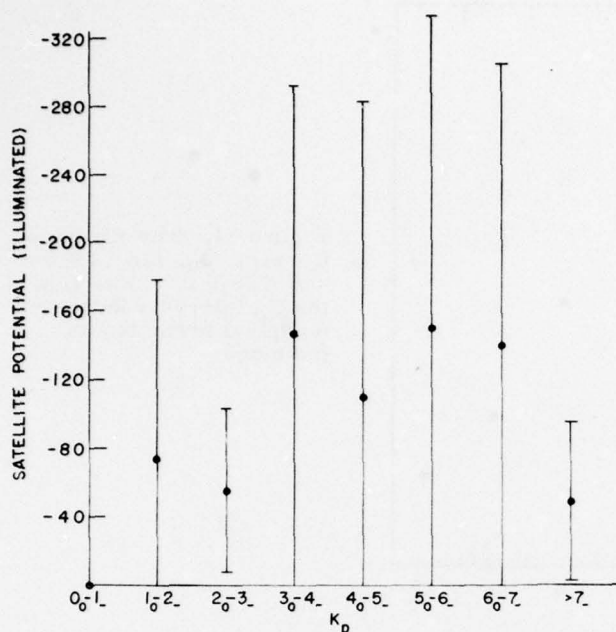
Figure 13. Averages of the Daylight Potential in the Indicated K_p Intervals Observed by ATS-6. Averages are only for non-zero values
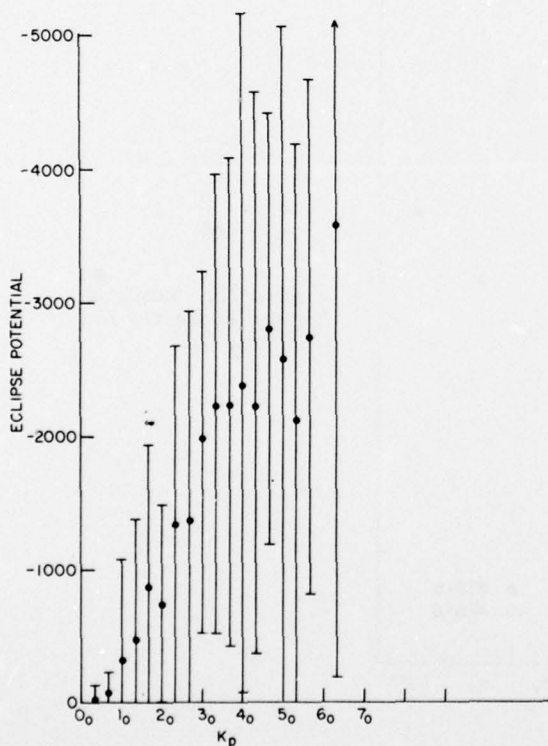
Figure 14. Averages of the Eclipse Potentials Observed by ATS-5 (1969-1972) and ATS-6 (1976) for the Indicated K_p Values. The eclipse potentials were the averages for each eclipse observed. Zero values were included

26

4.5 Current vs Temperature

The relationship between temperature and current is an important prerequisite for charging theory. Figure 15 is a contour plot of the temperature T(RMS) vs the current for ATS-5 electron observations. Figure 16 is the same plot for the ions (as the results for ATS-6 and for T(AVG) are nearly identical to those in Figures 15 and 16, we will only discuss the ATS-5, T(RMS) data). The ion contour plot shows essentially a random distribution around an average value whether T(RMS) or T(AVG) is considered. The electron data, on the other hand, show a distinct well shaped statistical profile in which there is a weak, but direct relationship between the current and temperature at high currents (that is, current increases as T(RMS) increases). Figure 17 is a "blow-up" of the lower left-hand corner of the T(RMS) plot demonstrating a strong inverse relation between the electron current and temperature at low current levels. In Section 5, this peculiar effect will be discussed in some detail.
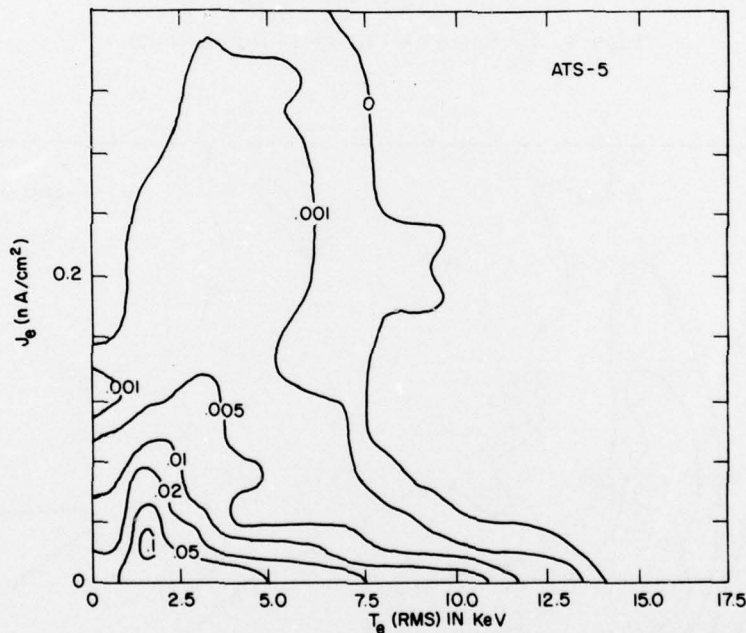
Figure 15. Contour Plot of Occurrence Frequency of Electron Current vs T(RMS) as Observed by ATS-5. Contours correspond to percentage of all 10-min intervals studied

27
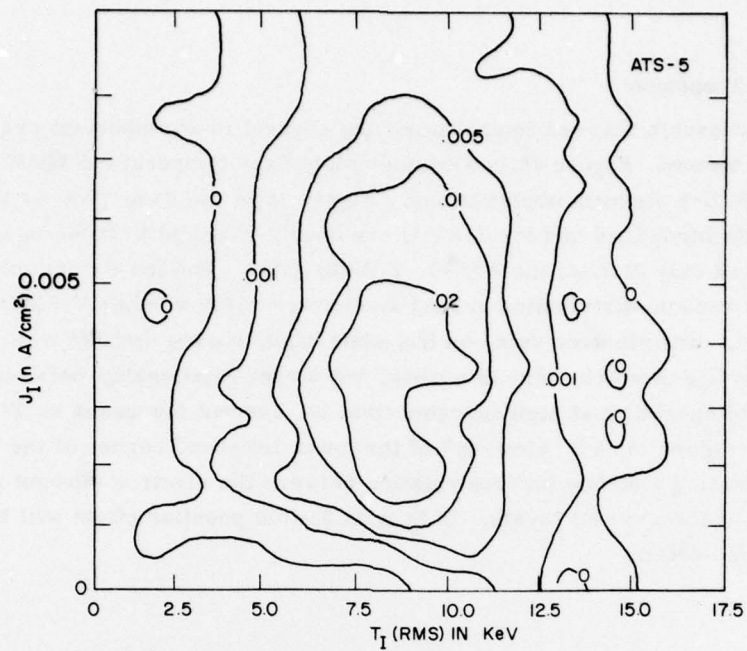
Figure 16. Same as Figure 15 for the Ions
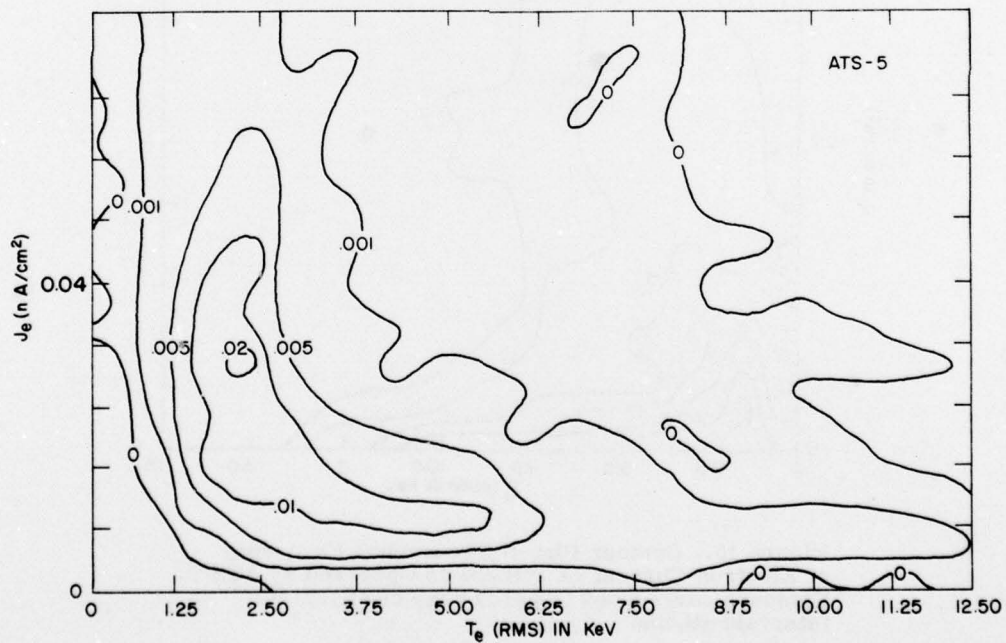
Figure 17. Same as Figure 15, Except for an Enlarged Section

28

5. DISCUSSION OF RESULTS

Our observations can be generalized as follows:

(1) $T(AVG) \sim 1/2 \cdot T(RMS)$,

(2) $T_{ATS-5} \sim 1/2 \cdot T_{ATS-6}$,

(3) $Potential_{ATS-5} \sim 1/2 \cdot Potential_{ATS-6}$ (for eclipse).

(4) T(RMS) peaks near 1200 local time,

(5) T(AVG) for ATS-6 and ATS-5 differ in their local time variation,

(6) Both electron and ion currents peak near midnight,

(7) Pronounced local time peaks in potential exist near midnight,

(8) T increases slightly for the electrons with K_p,

(9) Current (particularly electron current) increases with K_p,

(10) Potential (near midnight) increases with geomagnetic activity,

(11) A peculiar relation exists between electron current and temperature that is dependent on the range of the values discussed,

(12) Ion current and temperature are not correlated.

Although no theory we could currently advance would explain all of the above phenomena, a simple interpretation is possible in terms of well-known magnetospheric theory[12, 16] and charging theory. [10, 15]

The basic theory is illustrated in Figure 18 where we have presented a spectrogram from ATS-5 for December 1970 (see DeForest and McIlwain[17] for a detailed explanation). The features we desire to call attention to are:

(1) The plasma injection encountered near local midnight (0630),

(2) The rapid decay with local time of the flux,

(3) The high energy drifting particles or drift echoes following injection.

These three observations are fairly representative of most plasma injections.

The intense fluxes near midnight associated with the injection readily explains observation (6). Likewise, observation (9) also follows as injections are believed to be closely associated with increases in geomagnetic activity. As stated earlier, the fact that the magnetosphere can be greatly perturbed by geomagnetic activity accounts for the lack of an exact 1 to 1 correspondence.

As discussed by Roederer[16] and others, simple magnetospheric models indicate that as a result of particles drifting in the earth's magnetic field, the average particle energy or temperature increases slightly near noon [observation (4)]. This is not a

16. Roederer, J.G. (1970) Dynamics of geomagnetically trapped radiation, Physics and Chemistry in Space, Vol. 2, edited by J.G. Roederer and J. Zahringer, Springer, New York.

17. DeForest, S.E., and McIlwain, C.E. (1971) Plasma clouds in the magnetosphere, J. Geophys. Res. 76:3587:3611.

29

great percentage change—certainly not as great as the electron current exhibits in local time and should not be confused with plasma changes following an injection.
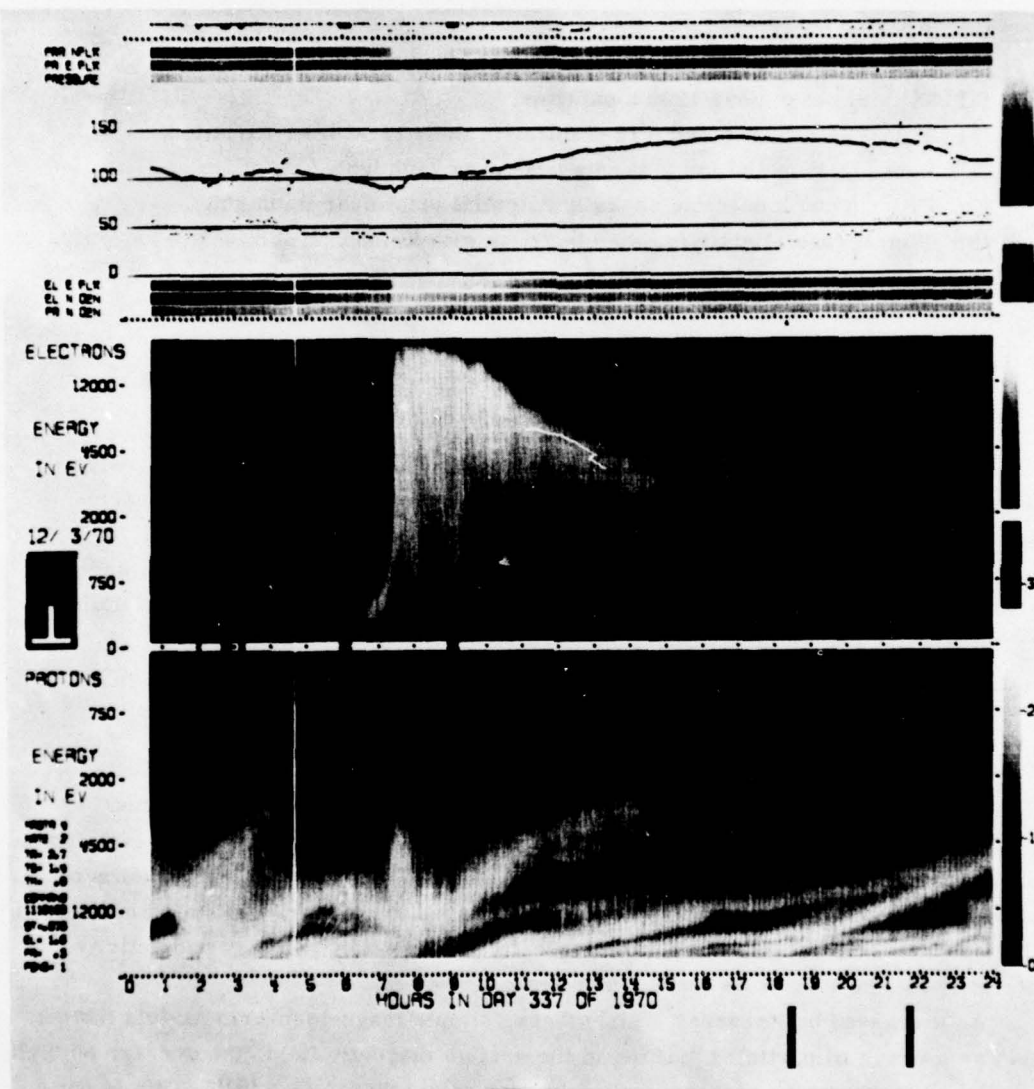
Figure 18. ATS-5 Spectrogram for Day 337, 1970 (3 December 1970) Illustrating Several Plasma Injections, Culminating in a Major Injection Near 0700 UT. Local midnight is at 0630 UT

Figure 19 is a qualitative plot of Figure 18. Basically, the flux (number or energy) varies in time with the characteristic pattern of Figure 18. The initial injection of particles near local midnight is approximately Maxwellian (see De-Forest[17] and Garrett and Rubin.)[10] This initial cloud rapidly disperses with the higher energy particles gradient drifting and the lower energy particles drifting or being convected away. At moderate energy (10-40 keV) the particles are rapidly lost due to these mechanisms and pitch angle scattering. Higher energy particles remain longer (~ 24 hr or longer), drifting around the earth in the so-called ring current. The low energy population appears to be either replenished or simply does not disperse very rapidly (we cannot tell in this simple model). These processes lead to two or more populations of particles from what was originally a single population. The effects of this division of the plasma population is crucial to our understanding of observation (1). A two Maxwellian distribution appears to adequately represent this division of the plasma in many cases. In fact, as previously discussed, distinct values of N1, N2, T1, and T2 exist that give the observed T(AVG) and T(RMS) average values and readily explain the factor of 2 difference between T(AVG) and T(RMS).
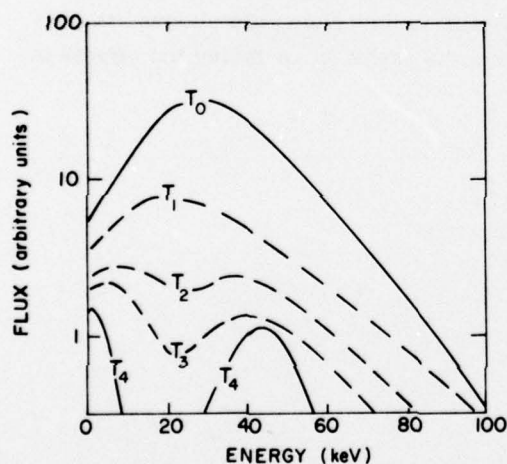
Figure 19. Qualitative Representation of the Evolution of the Particle Flux at Geosynchronous Orbit Following an Injection When the Satellite was Near Midnight

According to the model, the plasma at midnight following an injection is Maxwellian and at a high density for both the electrons and ions. As indicated in Figure 19, the population quickly evolves into 2 or more populations which are approximately equal in density for the ions (favoring somewhat the high energy component) but unequal for the electrons (favoring the low energy component). This difference in evolution of the electron and ion populations may explain the relationships

31

that exist between the currents and temperatures. This possibility is based on the fact that the current ($\sim NT^{1/2}$) is more dependent on the density than temperature. Initially, for the electron plasma, as the plasma is Maxwellian, an increase in either density or temperature increases the current. As time progresses, the temperature would increase [T(RMS)] or stay the same [T(AVG)] as the high energy component temperature (T2) increases, whereas the density falls rapidly accounting for the inverse relation between current and temperature. For the ions, the evolution into many, approximately equivalent temperature components could explain the lack of any relationship between the current and temperature.

6. CONCLUSION

In the preceding sections we have described the data base which was used in the study. Various difficulties in studying the data, particularly the inability of a single Maxwellian to adequately model the plasma were discussed. The data were then analyzed by statistical means. Variations in the current, potential, and temperature [T(AVG) and T(RMS)] were studied as functions of local time and K_p. An attempt was made to explain these variations in terms of a simple model of the evolution of the plasma following injection. Finally, although the study clearly indicates the inadequacies of T(AVG) and T(RMS) in describing the plasma, the results reported in the study should still prove to be useful in analyzing the effects of spacecraft charging.

32

References ·

1. Vasyliunas, V. M. (1968) A survey of low-energy electrons in the evening sector of the magnetosphere with OGO 1 and OGO 3, J. Geophys. Res. 73:2839-2884.

2. DeForest, S. E. (1977) Specification of the Geosynchronous Plasma Environment, AFGL-TR-77-0031.

3. Sy, S.-Y., and Konradi, A. (1977) Description of the plasma environment at geosynchronous altitude, NASA Johnson Technical Note, p. 10.

4. Garrett, H. B. (1977) Modeling of the Geosynchronous Orbit Plasma Environment - Part I, AFGL-TR-77-0288.

5. Lennartsson, W., and Reasoner, D. L. (1978) Low-energy plasma observations at synchronous orbit, J. Geophys. Res. 83:2145-2156.

6. Reasoner, D. L., Lennartsson, W., and Chappell, C. R. (1976) Relationship between ATS-6 spacecraft-charging occurrences and warm plasma encounters, Spacecraft Charging by Magnetospheric Plasmas, AIAA Progress in Astronautics and Aeronautics Series, Vol. 42.

7. Johnson, B., and Quinn, J. (1977) Correlation of plasma parameters with spacecraft charging on ATS6, EOS, 58:1215.

8. Johnson, B., Quinn, J., and DeForest, S. (1978) Spacecraft charging on ATS-6, Proceedings of the Symposium "The Effect of the Ionosphere on Space Systems and Communications", Washington, D.C.

9. Mauk, B. H., and McIlwain, C. E. (1975) ATS-6 UCSD auroral particles experiment, IEEE Trans. Aerospace and Electronics Systems, AES-11(No. 6):1125-1130.

10. Garrett, H. B., and Rubin, A. G. (1978) Spacecraft Charging at Geosynchronous Orbit-solution for Eclipse Passage, AFGL-TR-78-0122.

11. Mauk, B. H., and McIlwain, C. E. (1974) Correlation of K_p with the substorm plasma sheet boundary, J. Geophys. Res. 79:3193-3196.

12. McIlwain, C. E. (1972) Plasma convection in the vicinity of the geosynchronous orbit, in Earth's Magnetospheric Processes, edited by B. M. McCormac, p 268, D. Reidel, Dordrecht, Netherlands.

13. Roederer, J. G., and Hones, E. W., Jr. (1974) Motion of magnetospheric particle clouds in a time-dependent electric field model, J. Geophys. Res. pp 1932-1438.

14. Garrett, H. B., Pavel, A. L., and Hardy, D. A. (1977) Rapid Variations in Spacecraft Potential, AFGL-TR-77-0132.

15. Rubin, A. G., Garrett, H. B., and Rothwell, P. L. (1978) ATS-5 and ATS-6 potentials during eclipse, Proceedings of the Second Spacecraft Charging Technology Conference (to appear as AFGL/NASA publication).

16. Roederer, J. G. (1970) Dynamics of geomagnetically trapped radiation, Physics and Chemistry in Space, Vol. 2, edited by J. G. Roederer and J. Zahringer, Springer, New York.

17. DeForest, S. E., and McIlwain, C. E. (1971) Plasma clouds in the magnetosphere, J. Geophys. Res. 76:3587-3611.